An Improved SPICE Model for MEMS Based Capacitive Accelerometers

C. Kavitha*, M. Ganesh Madhan†

Department of Electronics Engineering, Anna University, M.I.T Campus, 600 044 Chennai, India

(Received 15 February 2013; revised manuscript received 29 April 2013; published online 04 May 2013)

An improved electrical equivalent circuit for a capacitive MEMS accelerometer, incorporating temperature, pressure and squeezed film effects is reported. The circuit model corresponds to a single degree of freedom (SDOF) vibrating system, including dominant micro physical mechanisms. Static, transient and frequency response analysis are carried out at temperature and pressure ranges of 100 K to 400 K and 30 to 3000 Pa respectively. The effect of these parameters on the resonance frequency, peak displacement and settling time of the accelerometer are determined. Simulations are performed using PSpice® circuit simulator.

Keywords: Squeezed film, Capacitive accelerometer, Thermal effect, Damping, Electrical attractive force.

PACS number: 85.85. + jx

1. INTRODUCTION

MEMS (Micro Electro Mechanical Systems) technology involves integration of mechanical, fluidic, optical and electrical components. The advantages are low cost and reduced size. Accelerometers are classified as piezoresistive, piezoelectric and capacitive types. Among all, the capacitive type is mostly preferred in commercial applications. Due to its high sensitivity, low noise and low power dissipation characteristics. In MEMS based accelerometer, the mechanical vibrations are converted to electrical signal by the sensing elements. The device performance depends on the elastic properties of silicon, capacitance and voltage measurements by electronic interface circuits. In MEMS accelerometers, gas is often employed as a damping medium, which has a significant impact on the accelerometer behavior. The compression of gas due to moving plates has to be carefully adjusted to obtain the desired response [1]. Usually the compressible gas films are analyzed using Reynolds equation [2]. This approach has been used by many authors to study the frequency response of micro mechanical pressure sensors [3-5]. Timo Veijola et. al. [6] has developed a circuit model that involves damping and spring forces created by squeezed film. They have determined the response of MEMS accelerometer using linear and nonlinear frequency dependent components, under different pressures. They have used a self developed circuit simulation program APLAC [7] for their analysis. In this paper, we report an improved circuit model based on Timo Veijola's approach, to study the effect of temperature and pressure on capacitive MEMS accelerometer. In our approach, the parallel resonator circuit model is replaced by variable inductor and resistor implemented as controlled current sources. This scheme also includes temperature and pressure dependent squeezed film and thermo elastic damping models. Based on this model the DC, Transient and frequency response analysis are carried out at different pressures and temperatures, using a commercial circuit simulator PSpice.

2. MEMS ACCELEROMETEER MODELING

A typical micromachined capacitive accelerometer [1, 8] consists of a mass suspended with a small cantilever beam which is located inside the cavity of a small silicon block. In the capacitive measurement scheme, the movement of the cantilever is measured as a change of capacitance between the plates above and below the cantilever. Acceleration acting on the cantilever alters the air gap dimensions leading to increase of capacitance in one side and decrease in the other side. The sensitivity of the capacitive accelerometers is determined by the Young's modulus, thermal coefficients of the materials and electronic interface circuit connected to the sensing element. Generally this accelerometer type is modeled as mass-spring-damper system and its corresponding schematic diagram is shown in Fig. 1. It consists of a proof mass, which is supported in such a way that it can move only in the *x*-direction, a spring, and a dashpot damper.

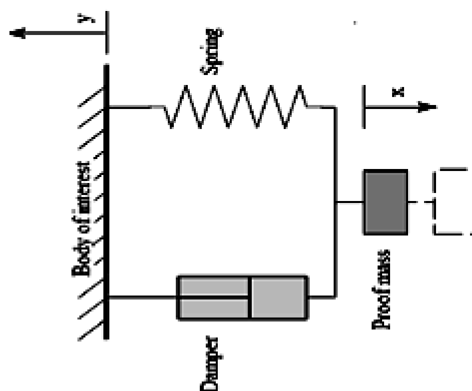

Fig. 1 – schematic diagram of single degree of freedom (SDOF) mechanical resonator

The dynamics of a simple accelerometer is characterized by the following differential equation

* kaviphd2011@yahoo.co.in
† mganesh@annauniv.edu

 © 2013 Sumy State University

$$M\frac{d^2x}{dt^2}+D\frac{dx}{dt}+kx=F_{ext}+F_{el} \quad (1)$$

The force (F) is the sum of an external mechanical force F_{ext} and an internal electrical attractive force F_{el}. The electrical attractive force on the mass is caused by the potential difference across the capacitor plates. Assuming the motion perpendicular to the plate surfaces, the electrostatic force is given as

$$F_{el}=\frac{\varepsilon AU^2}{2d^2} \quad (2)$$

where ε is the dielectric constant of the gas, A is the plate area, U is the capacitor voltage and d is the gap width. The mechanical accelerometer model is realized by the equivalent electrical model of a parallel resonator and is given by the differential equation as

$$C\frac{d^2\varphi}{dt^2}+\frac{1}{R}\frac{d\varphi}{dt}+\frac{1}{L}\varphi=I_{ext} \quad (3)$$

where C is the capacitance, φ is the flux, R is the resistance, L is the inductance and I_{ext} is the external current. The displacement equals, Li_L, where i_L is the current through the inductor.

2.1 Squeezed Film Effect

A Simple linear MEMS capacitive accelerometer model with viscous gas flow is considered. The structure consists of a mass with cantilever beams and two fixed electrodes [8]. The region between the electrodes may be filled by the damping medium such as gas or liquid. Due to vibrations of proof mass the gas flow in a narrow air gaps will cause damping [9, 10]. The gas pressure inside the sensor can be changed to control the squeezed film effect. The distribution of the gas pressure in the gap between two moving plates is governed by Reynolds equation for a compressible gas film [1, 2]. Assuming isothermal viscous flow behavior between flat surfaces, the linearized Reynolds squeeze film equation is given as

$$\frac{P_a d^2}{12\eta_{eff}}\nabla^2\left(\frac{p}{P_a}\right)-\frac{\partial}{\partial t}\left(\frac{p}{P_a}\right)=\frac{\partial}{\partial t}\left(\frac{x}{d}\right) \quad (4)$$

where P_a is the ambient pressure, η_{eff} is the effective gas viscosity, ∇^2 is the Laplacian operator, p is a small pressure change of P_a and x is a variation of the plate spacing. Continuum theory is valid for Knudsen numbers smaller than 0.01 and can be estimated by

$$K_n=\frac{\lambda}{d} \quad (5)$$

where K_n is the Knudsen number, $\lambda=P_o\lambda_o/P_a$ is a mean free path, λ_o is the mean free path at pressure P_o. To consider the slip flow boundary conditions, an effective viscosity is used for the systems to operate at high Knudsen numbers and this model is derived from Boltzmann equation and is calculated [11] by

$$\eta_{eff}=\frac{\eta}{1+9.638\left(K_n\right)^{1.159}} \quad (6)$$

where η is the viscosity coefficient. These above effects are realized with few Resistance-Inductance (RL) sections in the equivalent circuit representation of squeezed film effect.

$$L_{mn}=\left(mn\right)^2\frac{\pi^4 d}{64AP_a} \quad (7)$$

$$R_{mn}=\left(mn\right)^2\left(m^2+c^2n^2\right)\frac{\pi^6 d^3}{768Aw^2\eta_{eff}} \quad (8)$$

where L_{mn} and R_{mn} are inductance and resistance for the squeeze film on air gaps in both sides, which is represented as A and B in a model. m and n are odd integers 1, 3, 5 …. $A=wl$ is the rectangular plate area, $c=w/l$, w and l are the width and length of the mass respectively. Six sections are used in our simulations to model both air gaps with odd integers as $((m, n)=(1, 1), (1, 3), (3, 1), (3, 3), (1, 5), (5, 1))$.

The gas pressure also changes the squeeze number and is given by

$$\sigma=\frac{12\eta_{eff}w^2}{P_a d^2}\omega \quad (9)$$

where ω is the angular frequency. The accelerometer physical parameters are listed in Table 1.

2.2 Thermo Elastic Damping

As the temperature increases, Young's modulus and thermal expansion coefficient of silicon material (111) decreases and increases respectively [12, 13, 14 and 15]. This results in change of cantilever length, spring constant and resonant frequency.

Table 1 – Physical parameters of accelerometers [1]

Parameter	Value
Mass M	4.9 μg
Width of the moving mass w	2.96 mm
Length of the moving mass l	1.78 mm
Length of the cantilever beam	520 μm
Gap widths d_A and d_B	3.95 ± 0.05 μm
Mean free path λ at 1 atm	70.0 ± 0.7 nm
Viscosity coefficient η	22.6 ± 0.2 μNsm^{-2}

The increase in length of cantilever due to thermal expansion coefficient of silicon at different temperature is calculated by

$$\delta=L\alpha_L\Delta T \quad (10)$$

The above effects are presented in Fig. 2. and Fig. 3.

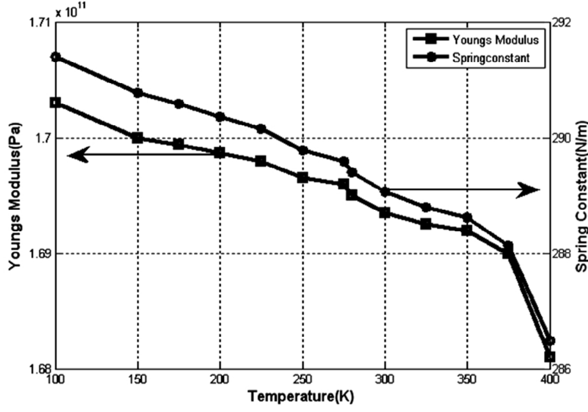

Fig. 2 – Thermal effect on stiffness and spring constant

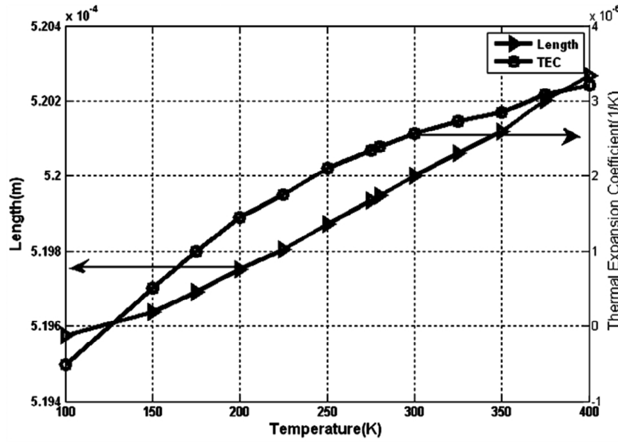

Fig. 3 – Temperature effect on length of cantilever and thermal expansion coefficient

Thermal strain and stresses can be estimated as

$$\varepsilon_T = \frac{\delta}{L} \tag{11}$$

$$\sigma_T = E\varepsilon_T \tag{12}$$

where ε_T is the Strain, σ_T is the stress, E is the Young's Modulus of silicon material. Moment of inertia of the cantilever is obtained by

$$I = \frac{bh^3}{12} \tag{13}$$

where b is the width and h is the thickness of the cantilever beam. As temperature increases, the spring constant reduces as per the following equation [9].

$$K = \frac{3EI}{L^3} \tag{14}$$

The elasticity coefficient variation with temperature also affects the resonance frequency by the relation

$$f_r = \frac{1}{2\pi}\sqrt{\frac{K}{M}} \tag{15}$$

The variation is shown in Fig. 4.

Viscosity (η) of a gas is altered by temperature as follows

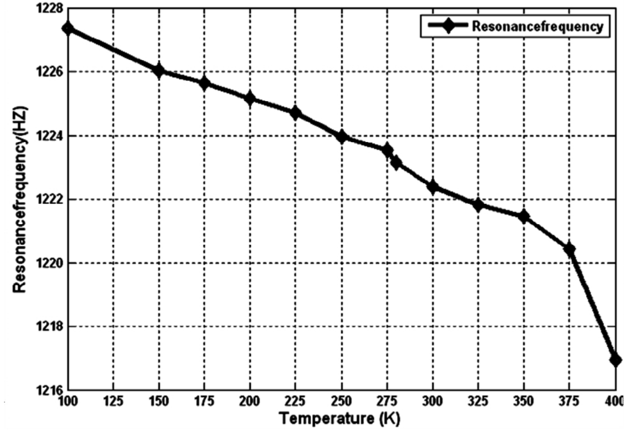

Fig. 4 – Thermal effect on resonance frequency for simple spring mass dashpot system

$$\eta = \eta_o\left(\frac{0.555T_o + C}{0.555T + C}\right)\left(\frac{T}{T_o}\right)^{3/2} \tag{16}$$

where η_o is the reference viscosity at reference temperature T_o, C is the Sutherland constant for the gas. The mean free path equation is

$$\lambda = \frac{RT}{\sqrt{2}\pi d_a{}^2 LP} \tag{17}$$

where R is a gas law constant, L is the Avagadro's number, T is the temperature in Kelvin, d_a is the collisional cross section, P is the Pressure. The mean free path dependence on temperature and pressure is shown in Fig. 5. The damping coefficient is evaluated by

$$D = \frac{2\eta Lb}{d} \tag{18}$$

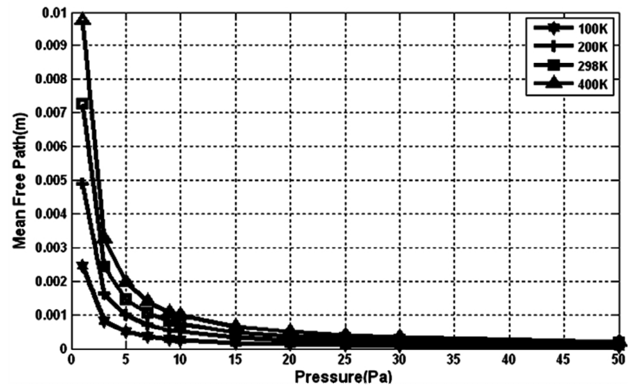

Fig. 5 – Temperature and pressure effect on mean free path

3. EQUIVALENT CIRCUIT MODEL

The electrical equivalent circuit is normally developed for the capacitive accelerometer [1] using parallel RLC circuit with two air gap sections in the form of parallel RL sections(squeezed film damping effects) [4, 6, 8 and 9]. In the proposed model temperature, pressure and bias voltage applied to the parallel plates are fixed as one unit and the equivalent circuit of accelerometer is kept as another unit, with mutual interaction between them. The block diagram is shown in Fig. 6.

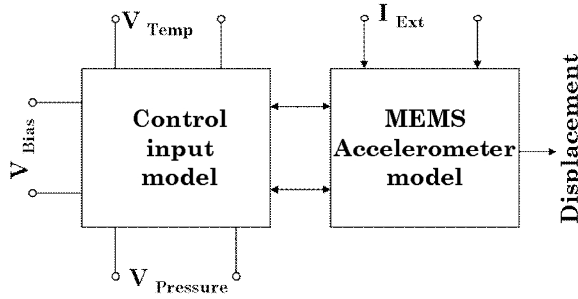

Fig. 6 – Modeling approach-block diagram

As temperature increases, the length of cantilever beam gets elongated which changes the inductance and resistance in the equivalent circuit, which represents spring constant and damping coefficient. The temperature is modeled as a voltage source in PSpice and all other effects are developed as voltage dependent voltage sources (VCVS). Temperature is varied in the range of 100 K to 400 K for the device under study. The thermal expansion coefficient and young's modulus values are evaluated by a second order polynomial, using curve fitting technique. They are implemented as a Voltage controlled voltage source (VCVS). The inductance and resistance values are found to vary in the range of 3.43 mH to 3.49 mH and 23.06 MΩ to 5.423 MΩ respectively, for temperature range of 100 K to 400 K. The pressure of the argon gas, considered as the damping medium, is also varied in the range of 30 Pa to 3000 Pa. The pressure parameter is assumed as a voltage source which affects the Knudsen number, dynamic viscosity and effective viscosity. The complete equivalent circuit developed is shown in Fig. 7.

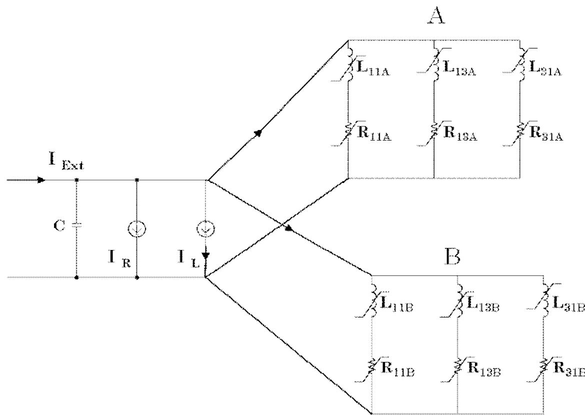

Fig. 7 – Electrical equivalent circuit for a temperature dependent nonlinear model of MEMS accelerometer

4. SIMULATION RESULTS

4.1 D.C. Response Analysis

Unequal bias voltages applied to the mass, creates a non uniform electrostatic force, which causes the displacement of the movable mass from the centre position. Because of unequal air gap lengths, the value of capacitance increases in one side and decrease in the other. These capacitance values are calculated by assuming the displacement only in x direction as

$$C_1 = \frac{\varepsilon A}{d_a - x} \tag{19}$$

$$C_2 = \frac{\varepsilon A}{d_b - x} \tag{20}$$

where C_1 and C_2 are capacitance between movable electrode and fixed electrode of two sides, ε is the dielectric constant of the gas in the air gap, A is the plate area, d_a and d_b are gap widths.

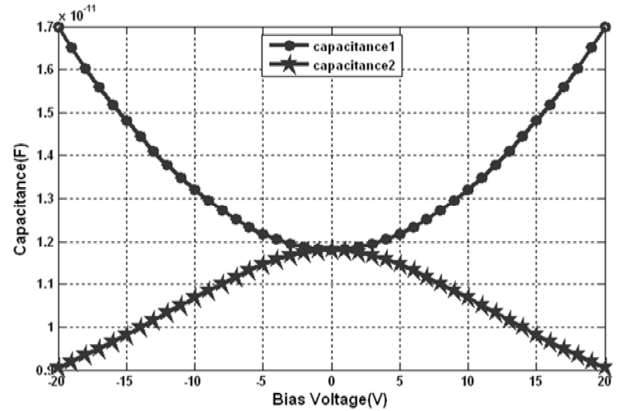

Fig. 8 – Plate capacitances with applied bias

Capacitance depends on air gap distance between plates and the bias voltage. Under symmetrical bias condition ($V_{bias1} = V_{bias2}$), the nominal capacitance value is obtained as 11.81PF.

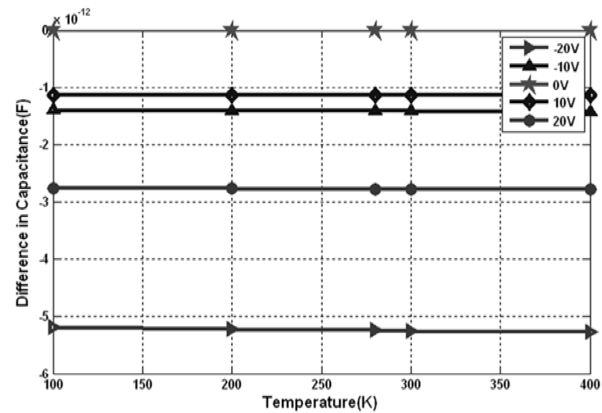

Fig. 9 – Temperature Vs Difference in Capacitance for different bias

$$F_{el} = \frac{\varepsilon A}{2} \cdot \frac{(V_{bias1})^2}{\left(d_a - x\right)^2} - \frac{\varepsilon A}{2} \cdot \frac{(V_{bias2})^2}{\left(d_b + x\right)^2} \tag{21}$$

where V_{bias1} and V_{bias2} are the voltages which are applied between movable and fixed electrodes. The capacitance change with bias voltage is shown in Fig. 8. We have estimated capacitance in the temperature ranges of 100 K to 400 K with and without squeeze film effect. It is observed that a pressure change does not affect the capacitance at constant temperature. Similar analysis is carried out for different temperatures at constant pressure exhibits variation in capacitance only at larger bias levels. The differences in capacitance under dif-

ferent bias conditions are shown in Fig. 9.

4.2 Transient Response Analysis

A step input current equivalent to an acceleration of 0.5g is applied to the movable mass and the simulation is carried out under pressures of 30 Pa, 300 Pa and 3000 Pa. Capacitance variations due to different pressures at two different temperatures 100 K and 400 K are shown in Fig. 10. and Fig. 11. The capacitance variation due to different temperatures at constant pressure is shown in Fig. 12. and Fig. 13. The transient analysis is carried out in the temperature range of 100 K and 400 K with different pressures.

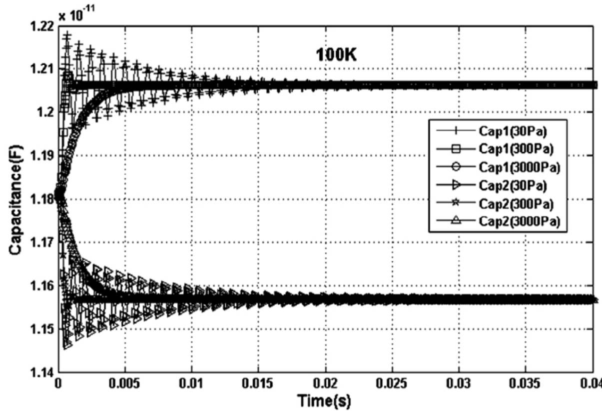

Fig. 10 – Capacitance variations without bias for 100 K

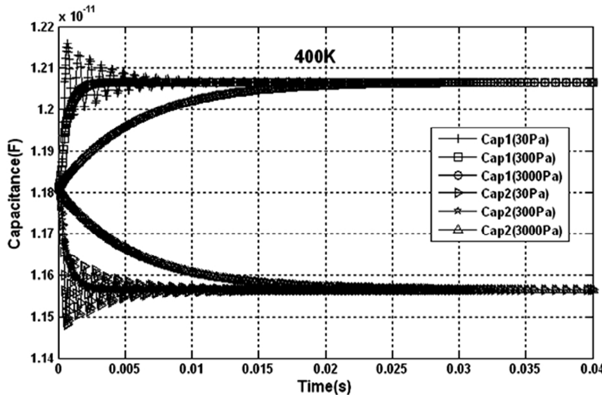

Fig. 11 – Capacitance variations without bias for 400K

Displacement of the proof mass under different pressure and temperature are shown in Fig. 14 and Fig. 15. At lower pressures, the displacement exhibits large oscillations. At 300 Pa, oscillations are reduced and reach steady state within few milli seconds. For 3000 Pa a large damping and increase rise time is observed. This increase damping, at high pressures is in accordance with the results of Timo Veijola and thus validates our model.

In the case of 100 K temperature and 30 Pa pressure, the displacement is found to be around 120 nm and settling time is around 30 ms. At pressures of 300 Pa and

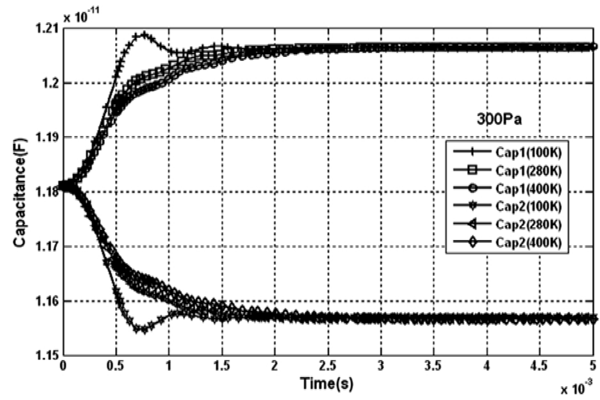

Fig. 12 – Capacitance variations without bias for 300 Pa

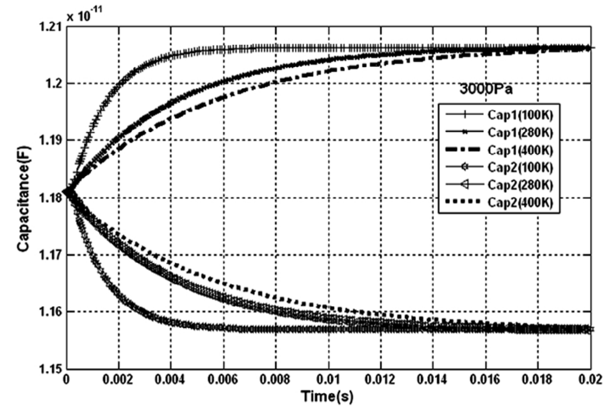

Fig. 13 – Capacitance variations without bias for 3000 Pa

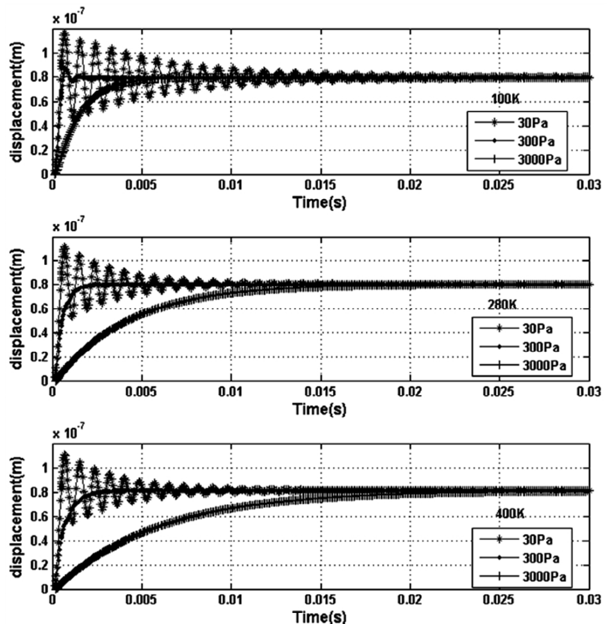

Fig. 14 – Transient analysis on displacement without bias for 100 K, 280 K and 400 K

3000 Pa, the displacement and settling time are observed to be 88 nm, 80 nm and 3 ms, 12 ms, respectively. For a constant pressure of 30 Pa with varying temperature of 100 K, 280 K and 400 K, the transient response shows a decreasing displacement and settling time. However, for 3000 Pa, the displacement and settling time is found to increase.

4.3 Frequency Response Analysis

An external ± 3 g force is applied to the mass of accelerometer and the displacement at each frequency is evaluated. If the bias voltages across the two capacitances are equal, the mass is restored to the original position. The analysis is repeated for different pressures and temperatures. The response is plotted in Fig. 16 and Fig. 17. Higher pressures lead to increased damping. Increase in temperature is found to affect the frequency response at higher pressures. The 3 dB bandwidth of the device is found to decrease with increasing pressure. The frequency response is more are less constant with temperature.

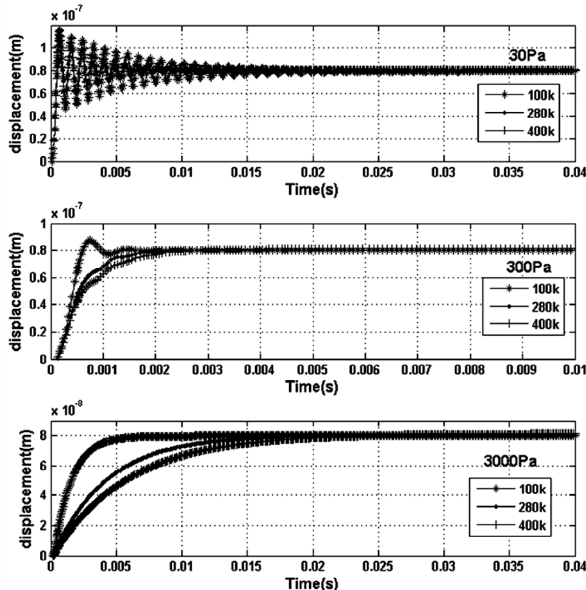

Fig. 15 – Transient analysis on displacement without bias for 30 Pa, 300 Pa and 3000 Pa

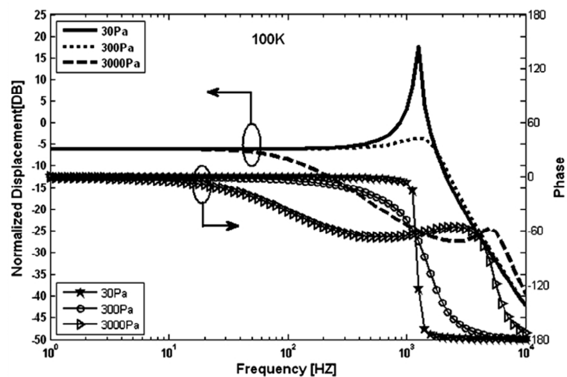

Fig. 16 – Frequency analysis on displacement for 30 Pa, 300 Pa and 3000 Pa at 100 K

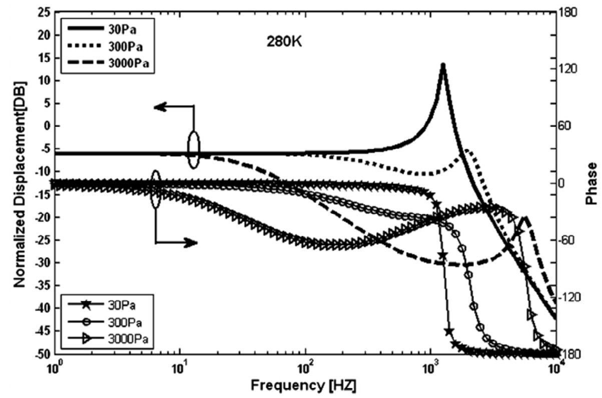

Fig. 17 – Frequency analysis on displacement for 30 Pa, 300 Pa and 3000 Pa at 280 K

The peak Displacement variation with temperature is shown in Fig. 18.

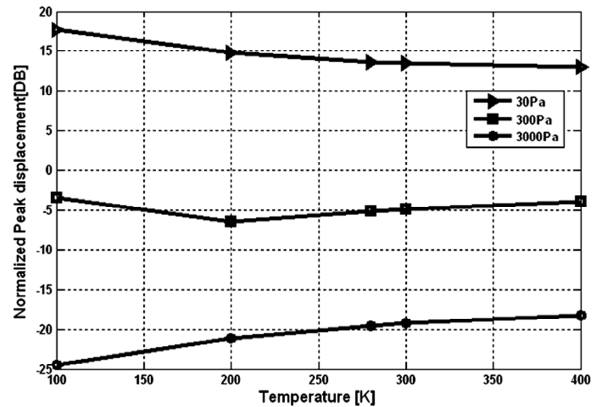

Fig. 18 – Peak displacement for 30 Pa, 300 Pa and 3000 Pa at different temperatures

5. CONCLUSIONS

An improved circuit model for capacitive MEMS accelerometer incorporating thermo elastic damping and squeezed film effects is developed. Based on this model temperature and pressure effects on the performance of accelerometer are studied, the developed model is compatible with PSpice circuit simulator.

ACKNOWLEDGEMENTS

The authors gratefully acknowledge Anna University, Chennai for providing financial support to carry out this research work under Anna Centenary Research Fellowship (ACRF) scheme. One of the authors, C.Kavitha is thankful to Anna University, Chennai for the award of Anna Centenary Research Fellowship.

REFERENCES

1. Timo Veijola, Heikki Kuisma, Juha Lhdenpera, Tapani Ryhanen, *Sensor. Actuat. A: Phys.* **48**, 239 (1995).
2. W.A. Gross, *Gas Film Lubrication* (New York: Wiley: 1962).
3. M.K. Andrews, G.C. Turner, P.D. Harris, I.M. Harris, *Sensor. Actuat. A: Phys.* **36**, 219 (1993).
4. M. Andrews, I. Harris, G. Turner, *Sensor. Actuat. A: Phys.* **36**, 79 (1993).
5. A. Sharma, M. Kaur, D. Bansal, D. Kumar, K. Rangra, *J. Nano- Electron. Phys.* **3**, No 1, 243 (2011).
6. W.S. Griffin, H.H. Richardson, S. Yamranami, *J. Basic Eng.-T ASME* **88**, 451 (1966).
7. T. Veijola, *Report CT-18* (Circuit Theory Laboratory, Helsinki University of Technology: Finland: 1994).
8. Timo Veijola, Heikki Kuisma, Juha Lahdenpera, *Proceedings of the 1998 International Conference on*

Modeling and Simulation of Microsystems – MSM'98, Santa Clara, 245 (Boston: Computational: 1998).
9. Timo Veijola, Tapani Ryhanen, *IEEE International Symposium on Circuits and Systems – ISCAS'95, 664* (Piscataway, NJ: IEEE: 1995).
10. C. Bourgeois, F. Porret, A. Hoogerwerf, *The 1997 Internafional Conference on Solid-State Sensors and Actuators – Tranducers'97 Chicago, 1117* (Piscataway, NJ: IEEE: 1997).
11. S. Fukui, R. Kaneko, *J. Tribol-T. ASME* **110**, 262 (1988).
12. M.J. Edwards, C.R. Bowen, D.W.E. Allsopp, A.C.E. Dent, *J. Phys. D: Appl. Phys.* **43**, 385502 (2010).
13. Gang Dai, Mei Li, Xiaoping He, Lianming Du, Beibei Shao, Wei Su, *Sensor. Actuat. A: Phys.* **172**, 369 (2011).
14. Jeung-Hyun Jeong, Sung-Hoon Chung, Se-Ho-Lee, Dongil Kwon, *J. Microelectromech. Syst.* **12**, 524 (2003).
15. Jing Wang, Qing-An Huang, Hong Yu, *J. Phys. D: Appl. Phys.* **41**, 165406 (2008)